

An image-based deep learning network technique for structural health monitoring

Dong-Han Lee^a and Bong-Hwan Koh*

Department of Mechanical, Robotics, and Energy Engineering, Dongguk University-Seoul,
30 Pildong-ro 1 gil, Jung-gu, Seoul 04620, Republic of Korea

(Received April 15, 2021, Revised September 24, 2021, Accepted September 27, 2021)

Abstract. When monitoring the structural integrity of a bridge using data collected through accelerometers, identifying the profile of the load exerted on the bridge from the vehicles passing over it becomes a crucial task. In this study, the speed and location of vehicles on the deck of a bridge is reconfigured using real-time video to implicitly associate the load applied to the bridge with the response from the bridge sensors to develop an image-based deep learning network model. Instead of directly measuring the load that a moving vehicle exerts on the bridge, the intention in the proposed method is to replace the correlation between the movement of vehicles from CCTV images and the corresponding response by the bridge with a neural network model. Given the framework of an input-output-based system identification, CCTV images secured from the bridge and the acceleration measurements from a cantilevered beam are combined during the process of training the neural network model. Since in reality, structural damage cannot be induced in a bridge, the focus of the study is on identifying local changes in parameters by adding mass to a cantilevered beam in the laboratory. The study successfully identified the change in the material parameters in the beam by using the deep-learning neural network model. Also, the method correctly predicted the acceleration response of the beam. The proposed approach can be extended to the structural health monitoring of actual bridges, and its sensitivity to damage can also be improved through optimization of the network training.

Keywords: damage detection; deep learning; structural health monitoring; system identification

1. Introduction

The dynamic load caused by vehicles passing over a bridge can induce structural damage to its structure over a long period of time that can grow in severity in an unpredictable manner. Delaying repairs to critical damage in a bridge can lead to a catastrophe whereby part or all of the bridge collapses. To prevent this, structural health monitoring technology to assess the integrity of the bridge is an essential activity in the maintenance and management of a bridge system. To this end, structural integrity evaluation and monitoring techniques are continually being developed to diagnosis the condition of bridge structures and confirm the need for maintenance and repair.

From a monitoring perspective, data can be collected using a number of sensor networks (Lynch *et al.* 2004, Jang *et al.* 2010), such as acceleration (Meng *et al.* 2007, Yi *et al.* 2013) and optical fiber (Enckell *et al.* 2011, Mufti *et al.* 1997) sensors to detect vibrations and deformation due to applied loads to a bridge (Cho *et al.* 2010). Although employing multi-functional or heterogeneous sensors to monitor a bridge has the advantage of providing a variety of information items to assess the location, severity, and characteristics of a damaged area in a bridge, the sensitivity

of each one can be uneven, making it difficult to combine their outputs for decision-making. Moreover, deploying large-scale sensors is very limited in practice because additional work such as utility verification is required, which increases the operating cost. Therefore, methods for monitoring the integrity of a bridge system using a limited number and types of sensors will most likely be welcomed.

Xiao *et al.* (2019) performed parameter identification of truss members using a genetic algorithm and simulated annealing method through data measured from a limited number of strain gauges and displacement sensors to assess deformation in truss bridges. In addition, Comanducci *et al.* (2015) used data from sensors for monitoring vibrations in a bridge naturally caused by earthquakes or wind. They measured variations in wind speed using a novel detection method to identify any changes in the cables of a suspension bridge and constructed an analysis model to determine changes in the natural frequency of the suspension bridge using a principal component analysis. Smyth *et al.* (2003) used data from accelerometers installed on the Vincent Thomas suspension bridge from the Whittier Narrows earthquake in 1987 and the Northridge earthquake in 1994 to performed system identification of the corresponding bridge. The dynamic characteristics variations that occurred in the bridge during the two earthquakes were evaluated through an analysis of the natural frequency and damping changes.

Since earthquakes or high winds occur irregularly, they may be inappropriate for reliable monitoring strategies for

*Corresponding author, Ph.D., Professor,
E-mail: bkoh@dgu.ac.kr

^a Ph.D., E-mail: dh.lee@dgu.ac.kr

bridge systems that require constant monitoring. Therefore, monitoring methods by utilizing vibration data due to vehicles passing over the bridge are being developed (Moreu *et al.* 2017, Vagnoli *et al.* 2018, Malekjafarian *et al.* 2015, Mei and Gül 2019). In this regard, the exact locations of individual vehicles passing over a bridge require tracking information such as speed and acceleration in real-time. To this end, low-powered Internet of Things (IoT) devices for monitoring the mechanical interaction between the bridge structure and the vehicle passing over it have been developed (Tong *et al.* 2019). Moreover, a study has been conducted to monitor a bridge system by independently and continuously measuring the vibrations caused by a heavy truck moving on the bridge while limiting the access of other vehicles (Deng and Cai 2009). Likewise, a sensor was attached to a bus passing over the bridge on a regular basis to collect long-term operational data (Miyamoto *et al.* 2017). In a similar study, data measured in real-time after establishing a wireless sensor network system in a truck passing over a bridge has been used to monitor the condition of the bridge (Hou *et al.* 2015). In addition, a small wireless mobile robot that can vertically climb to a location in the steel structure of the bridge where human access is difficult has been used to collect data (Zhu *et al.* 2012). The bridge system was identified by operating multiple mobile robot sensors to collect the response of the bridge.

To accurately determine the impact of an object of interest, such as a vehicle passing over a bridge, it is necessary to measure the force and friction applied to the contact point between the vehicle and the bridge deck. Although it is relatively easy to obtain the position and speed of a vehicle from a sensor installed inside the vehicle, it is difficult to collect them from outside of it in practice. Therefore, studies have been conducted to remotely estimate the dynamic state of vehicles on bridge decks (Hata and Wolf 2016, Byun *et al.* 2015, Kim and Park 2020). In this regard, studies have been performed to solve the inverse problem, i.e., finding the load applied to the bridge from the estimated vehicle position and speed (Deng *et al.* 2018, Cantero *et al.* 2017, Cantero *et al.* 2016). Nayek and Narasimhan (2020) focused on extracting contact-point responses for vehicles with multiple degrees of freedom passing over a bridge and reconstructing them with a Gaussian process latent force model. Khuc and Catbas (2018) estimated the location of a vehicle passing over a bridge using data collected from surveillance cameras; they employed a tracking technique based on Adaboost and Cascade classifiers and applied it for damage detection in a reduced model of the bridge.

With the recent enrichment of image processing and deep learning algorithms, many studies have been conducted to improve the quality of estimating the position and speed of a vehicle passing along a road (Goodfellow *et al.* 2016). Javadi *et al.* (2019) calculated the probability density function for localizing vehicles by using intrusion detection that isolates the moment of a vehicle passing by a specific location from CCTV images for traffic analysis. This technique estimates the speed of a vehicle, which was verified by comparing it with the GPS tracking data from

inside the vehicle. Luvizon *et al.* (2016) proposed a method for estimating a vehicle's speed through the extraction and tracking of vehicle feature points from images captured by CCTV installed on public roads. Sochor *et al.* (2017) extracted object-matching data for a vehicle in the form of a 3D box through the vanishing point in an image frame to improve the accuracy of speed measurements with a CCTV camera, and they also developed an automated camera calibration technique. Zhang *et al.* (2020) proposed a context-aware traffic surveillance system that incorporates sensor cues from autonomous vehicles. Pan *et al.* (2019) collected images of bridge structures using UAV (unmanned aerial vehicle) and generated point clouds of the bridge. Using this point clouds, they performed voxelization of the bridge and reconstructed the 3D model for monitoring the surface condition of the bridge. Jahanshahi and Masri (2012) employed 2D images through a robotic system and reconstructed 3D models to visually evaluate the state of the structure. In the study, they extracted features of cracks from the surface of structures composed of 3D models and used them to monitor the depth of cracks. Also, Yu *et al.* (2021) proposed YOLOv4-FPM, a deep learning model for multi-scale segmentation for real-time monitoring of cracks in bridges using UAV. In that study, crack locations were extracted in real time from images with cracks in complex backgrounds. Yang *et al.* (2019) proposed a deep learning model for plate number recognition based on a convolutional neural network (CNN) for vehicle speed measurement from a binocular stereo vision system; they performed stereo matching of camera images and developed a function for identifying the location of the vehicle on camera. Guo *et al.* (2020) used a self-organized clustering technique involving a Kohonen network and the long-short-term memory (LSTM) model on data collected from sensors on a bridge over a long period of time to evaluate the integrity of the bridge. They also predicted deflection detection of the bridge structure by using time series data from the LSTM network and compared these results with actual damage caused by deformations of the bridge structure. Although there exist many meaningful studies using surrogate models when it is difficult to employ real structures such as bridges for a test bed, a methodology that potentially uses the traffic video information of the bridge for its structural health monitoring is not available so far.

In this study, we propose a novel method to correlate a model for vehicle motion estimated from CCTV video images from a bridge to assess a change in mass in the cantilevered beam in the laboratory. The underlying idea is to define a neural network model that can link the responses from varying structural properties in the lab-scale system with a stream of video images containing vehicles passing on the bridge deck. To this end, the location of the vehicle was first extracted using object detection from image processing techniques. A conversion equation was then introduced to correlate the load applied to the bridge with the vehicle's position and speed. To accommodate the equivalent correlation model, an experiment was conducted to generate a force profile and use it as the input for the cantilevered beam structure in the laboratory. The acceleration response of the beam with and without mass

perturbation was subsequently collected. A CNN model (Goodfellow *et al.* 2016) for a cantilevered beam system that employs images of vehicles as input and acceleration measurement as output was developed to perform state-space system identification. Arbitrary changes in the mass of the cantilevered beam were successfully classified by using the results of system identification and the image-based neural network model, meaning that the lab-scale cantilevered beam system can easily be used to assess damage in a real bridge structure with sophisticated monitoring equipment.

2. The proposed method

An artificial neural network model is proposed to detect structural damage in bridge structures using video information of passing vehicles obtained from image acquisition devices installed on the bridge. In general, a vehicle passing over a bridge at high speed applies a dynamic load to the structure. The position and speed of the vehicle identified in the CCTV images were confirmed through object detection, and based on this, a synthesized load was applied to a cantilevered beam mounted on the laboratory floor. Since it is impossible to create meaningful structural damage to the actual bridge in practice, the movement of a vehicle collected through video cameras installed on the bridge and the dynamic load transmitted by the vehicle to the bridge was virtually reconstructed through simulation. More specifically, an equivalent experiment was conducted remotely by simplifying the dynamic load transmitted by the vehicle to the bridge as a load function over time, which was then applied to the cantilevered beam.

To realize damage to the bridge, its occurrence is simulated by adding mass to the original beam. The proposed method of correlating the image of the vehicle on the actual bridge with its presence on the simplified beam structure was verified in the proof-of-concept stage. Therefore, the procedure validated through this study can be readily applied by utilizing the data measured from the sensors installed on the actual bridge. We designed and trained a deep learning model to determine whether a change in mass occurred or not by associating the acceleration measurements from a sensor attached to the beam and the CCTV video images from the actual bridge structure. Ultimately, we would like to produce a technique that can monitor the damage that occurs to a bridge by assessing the CCTV images from the actual bridge and the vibration response of the accelerometer installed on the bridge on a real-time basis.

2.1 System identification for a surrogate beam model

To apply a system identification method (Imai *et al.* 1989, Juang 1994, Ljung 2010, Nagarajaiah *et al.* 2008) that generates a mathematical model of the physical system using input and output data, the time-history of the loads due to multiple vehicles passing over the bridge and their positions and speed should be known *a priori*. In the case of

a large-scale bridge in service, it is impossible to restrict or control the traffic so that an experiment on system identification can be conducted. Output-only based methods, which comprise one of the approaches for monitoring the structural integrity of a bridge without knowing the exact vehicle location and speed, have been applied in previous studies (James *et al.* 1995, Yang *et al.* 2016, Chang and Pakzad 2013). That is to say, the load used for the input is assumed to be random and the technique for monitoring the state of the system only uses the output information. However, for output-only based system modeling, white noise input is often assumed since the input for a physical system such as a bridge cannot be measured. Therefore, information used for a direct correlation of the input from a vehicle on the bridge with regards to the physical properties of the bridge is inevitably insufficient.

The model for the beam structure installed in the laboratory was obtained in the form of state-space representation using two observer/Kalman filter identification (OKID) techniques, ERA-OKID (Juang 1994) and ERA-OKID-Output-Only (Chang and Pakzad 2014). The critical step of developing a mathematical model for training neural network is to obtain a high-fidelity state-space representation from OKID. During the identification process, inevitably, a significant level of model reduction is required to satisfy both affordable number of states and acceptable qualities of validation between the model and measurements. We tried multiple cases having different number of states and compared those results with the performance of system model. We found that the model with 160 states provides the best result both in output estimation and damage detection.

Table 1 Eigenvalues and modal frequencies for the discrete-time system matrix from the FEM and estimated ones via the ERA-OKID and ERA-OKID-Output-Only methods

Identified Mode	FEM	ERA-OKID	ERA-OKID Output-Only
1	0.9999±0.0081j (6.45 Hz)	0.9978±0.050j (39.81 Hz)	0.9998±0.0086j (6.84 Hz)
2	0.9981 ± 0.0507 (40.46 Hz)	0.9901±0.1383j (110.42 Hz)	0.9978±0.0142j (11.27 Hz)
3	0.9849 ± 0.1411j (113.25 Hz)	0.9639±0.2621j (211.30 Hz)	0.9997±0.0356j (28.34 Hz)
4	0.9429 ± 0.2697j (221.68 Hz)	0.9090±0.4089j (336.37 Hz)	0.9988±0.0399j (31.74 Hz)
5	0.8497 ± 0.4202j (365.46 Hz)	0.9031±0.4276j (351.90 Hz)	0.9990±0.0441j (35.11 Hz)
6	0.6885 ± 0.5592j (542.86 Hz)	0.8133±0.5762j (490.51 Hz)	1.0005±0.0479j (38.05 Hz)
7	0.4640±0.6389j (750.18 Hz)	-0.1265±0.985j (1351.62 Hz)	0.9960±0.0507j (40.44 Hz)
8	0.2181±0.6171j (979.65 Hz)	-0.4700±0.8796j (1640.49 Hz)	0.9896±0.1377j (109.99 Hz)

Moreover, the discrete-time eigenvalues and modal frequencies for the system matrix obtained from a finite element model (FEM) and estimated by both ERA-OKID and ERA-OKID-Output-Only are reported in Table 1. For this, the dimensions of the aluminum beam structure were 1.1 m long, 0.1 m wide, and 0.01 m thick, and it had a modulus of elasticity of 69.0 MPa and a density of 7970 kg/m³. The load used as input for the structure was generated based on the CCTV image information, which is explained in the next section. The eigenvalues corresponding to modes 1 to 4 of the system matrix estimated with ERA-OKID using both the given input and output captured by the accelerometer were $0.9978 \pm 0.050j$, $0.9901 \pm 0.1381j$, $0.9639 \pm 0.2621j$ and $0.9090 \pm 0.4276j$ respectively. In addition, the unique values obtained through the ERA-OKID-Output-Only system identification for modes 7 to 8 were $0.9960 \pm 0.0507j$ and $0.9896 \pm 0.1377j$ respectively. Thus, it can be seen that a mode generated by an external input rather than an intrinsic value of the actual structure appears in modes 2 to 6. These eigenvalues can be attributed to the impedance of the input characteristics generated when the load is transmitted to the beam from the stinger of the electromagnetic shaker. Note that only four and three physical modes (bold letters) were identified through ERA-OKID and ERA-OKID-Output-Only method, respectively. As a result, it may be difficult to uniquely classify the modal components in the identified system, which may hinder the ability to detect damage based on damage-induced variation in the modal properties. This is caused by the fidelity of the overall system identification model being affected by the method and structural characteristics of the sensor input.

2.2 CCTV images of vehicles and acceleration measurements of a cantilevered beam

Thus, we tried to solve the problem with the conventional input/output-based identification method mentioned above. Specifically, we designed a deep neural network model to replace the CCTV image information as the input for the system. The actual force applied to the cantilevered beam structure is developed by the position and speed of the vehicle appearing in the CCTV images. Once again, many studies have been conducted to estimate this information from CCTV images (Tang *et al.* 2018, Dong *et al.* 2019, Li *et al.* 2019), and based on this research, a neural network model was constructed to solve the problem of low accuracy and reliability of input information by combining the surveillance CCTV images from a large bridge and the acceleration sensor measurements in the actual bridge structure.

Vibration is generated by a load caused by a vehicle passing over a bridge, and a mathematical model for the bridge can be obtained using the acceleration measurements from the sensor. Here, the input load is derived from a real-time video of a passing vehicle. To this end, a neural network model including video information as input was constructed, as shown in Fig. 1. First, preliminary work was performed to generate correlations between the CCTV images of the bridge and the responses of the structure. Using an object detection technique, the position of the

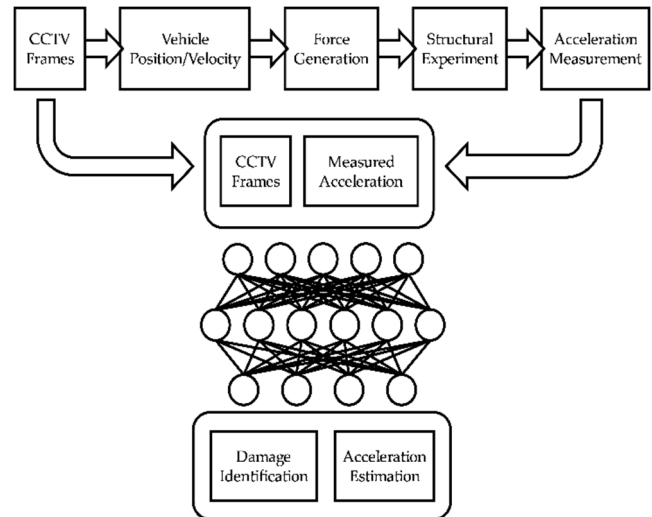


Fig. 1 An overall schematic of the proposed deep learning-based structural damage monitoring system through the fusion of CCTV video and acceleration measurements

vehicle passing over the bridge from CCTV images was estimated from a time series of positional changes over time (Papageorgiou and Poggio 2000, Redmon and Farhadi 2018). The corresponding speed was estimated for each vehicle or object based on the change in the position of the vehicle acquired from the image information over time. Here, using the estimated position and speed, an equation that simulates the force or input applied to the bridge was established, and the generation of force corresponding to the input of the bridge structure was calculated at the specific point where the vehicle passed.

Although the bridge structure and the beam are qualitatively or physically different, it is possible to conduct a methodological study by assuming an equivalent physical object. That is, the proposed method can be verified in that the response of the system to the applied load and the overall dynamic characteristics of the system are changed by local parameter changes or occurrence of damage. Hence, an equivalent experiment was performed on a cantilevered beam structure in the laboratory. An input load generated from a CCTV video was exerted on the beam structure through an electromagnetic shaker, and its vibration response was measured through an accelerometer attached to the beam. When damage occurs in a bridge structure, its stiffness and other physical properties change locally in response to the damage in various ways. To simulate this, an experiment was conducted to measure changes in the dynamic characteristics of the system by attaching an additional mass to a specific location on the laboratory beam and assuming that it had been damaged. The response by the beam structure when assuming that damage had been inflicted was also obtained through an FEM simulation and experimentation using the actual beam structure with identical dimensions. The acceleration response obtained through both simulation and experimentation was also collected. Given the difficulty of accessing sensor measurements from an operating bridge having real damages, the present work does provide enough

of a step forward to justify employing traffic video information for monitoring the structural integrity of a surrogate structure in laboratory. At this point in time, this study is not ready to undertake a real bridge verification beyond the proof-of-concept experiment.

A load profile generated from video from CCTVs installed on a specific bridge was applied to the beam in the laboratory, and these responses were used to construct a dataset for training an artificial neural network model. In addition, artificial neural network layers were developed for damage detection and response prediction based on the collected data. Once again, the force generated from the CCTV images of the bridge structure was applied as the input load for the beam, and a neural network model was devised to detect the damage and predict the response of the beam. We tried to confirm that the real-time CCTV video streaming data obtained from the bridge can be used for structural health monitoring and response prediction for the bridge.

2.3 Developing a deep-learning neural network model

A neural network model for system identification was constructed using the output obtained through the excitation experiment on the cantilevered beam installed in the lab and CCTV video of the vehicle passing over the deck of a bridge. The neural network inputs were composed of 0.2 seconds of video (equivalent to 12 frames) and acceleration signals (1000 data points). The output from the network comprised acceleration measurements (50 samples) that appeared at a later timestamp than the measured acceleration. The network output also included one of two beam condition states: healthy or a structural parameter change caused by adding extra mass to a specific point on the beam. A neural network model was constructed that performs two roles: estimating the acceleration over time after the measured acceleration on the laboratory beam and estimating the damage state of the beam.

A schematic diagram of the proposed neural network model is depicted in Fig. 2. Twelve CCTV video frames were processed as input on the convolution block composed of convolution (Conv), pooling (Pool), and batch normalization (BN) layers (three convolution blocks were used in this study).

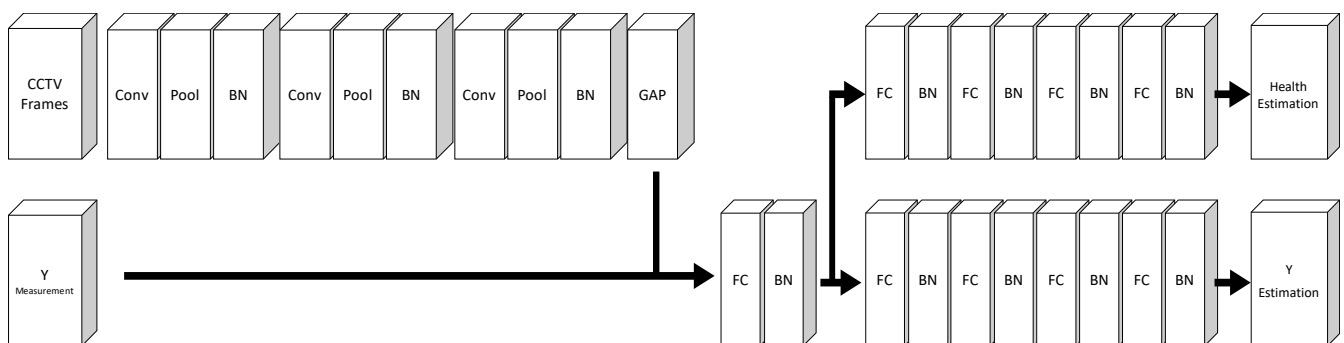


Fig. 2 Schematic diagram of the deep neural network model to process CCTV images and acceleration measurements for predicting the response and assessing the structural health of the bridge

The values from the convolution blocks were transformed into data items of $1 \times 1 \times \text{filter size}$ in the last layer. The value of the last convolution layer and the acceleration data were combined using a concatenation layer. In addition, a fully connected (FC) layer and the BN layers consist of four layers each. The implementation was divided into two parts: a network for predicting the structural health condition and a network for predicting the acceleration output of the system. Each FC layer was used by setting the filter size to decrease the values, i.e., from 1024 and 512 to 256 in alignment with reducing the large-dimensional data coming through the input into the final two binary values. In addition, the learning speed and stability were improved by using the BN layer between the FC layers. Thus, the network architecture used in this study comprises a CNN + FC structure: the CNN structure for processing image information and the FC structure for predicting fault conditions and system acceleration values from the measured acceleration data.

3. Experiments

Here, the procedure for object detection used to simulate the force input to a structure generated from CCTV images of a vehicle passing over a bridge is explained. The velocity of a vehicle in the CCTV videos was estimated using its positional changes in a time series comprising the frames. The profile of the input for the structural health assessment was generated using snapshots of vehicle positions and speed. The generated force creates a correlation between the image information and the structural dynamics.

3.1 Vehicle speed estimation based on object detection

Vehicles passing over a bridge apply various types of dynamic loads to the bridge according to the specific magnitudes of its mass, speed, and duration. Furthermore, the bridge structure responds to these inputs by vibrating. Therefore, if the dynamic behaviour of a vehicle passing over a bridge can be quantified, the position, shape, and range of the load applied to the bridge can be quantitatively determined. To this end, the object detection algorithm YOLOv3, commonly used in machine vision, was

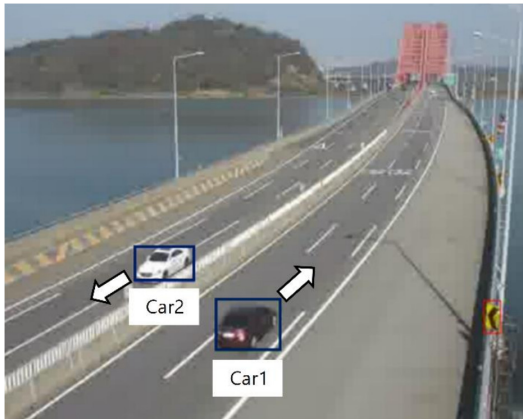


Fig. 3 Locations and directions of vehicles on the bridge identified through YOLOv3

employed to estimate the position and speed of a vehicle (Redmon and Farhadi 2018).

YOLOv3 is a neural net-based algorithm developed for multi-object detection and is used to estimate the position and size of an object by using three different image scales simultaneously based on the CNN structure. The position and size of the object recognized through the algorithm are tagged, and the object is output in the form of labelled data. Each recognized object contains the x and y -coordinates of the object on the image and the width and height of the area occupied by the object. When the image frame is treated as a time-related value, the size of the target object can be estimated and its speed in the image can be obtained through positional and time stamping. In this study,

YOLOv3 was used as the input load applied to the bridge by estimating the position change and size of an arbitrary vehicle passing over the bridge from acquired CCTV video. In Fig. 3, the position, direction, and size of the two cars estimated through YOLOv3 are objectized and depicted in a boxed frame.

Figs. 4(a) and 4(b) show the location of Car 1 in the CCTV image in Fig. 3 as x and y coordinates, respectively. When the vehicle estimated from the image is tracked and connected according to the change in each image frame, it appears that the vehicle speed can be obtained through the slope of this line, as depicted in Figs. 4(c) and 4(d). As the vehicle passes through the bridge, it generates a force that causes vibrations within the bridge. By interpreting this relationship as a system with input and output, the relationship between the bridge and the individual vehicles passing over it can be implemented as a dynamic model. In general, acceleration sensors are installed in various positions and orientations on a bridge, and the dynamic behaviour of the bridge is collected and monitored through powerful data acquisition systems.

The inputs to the configured network model are twelve-frame images for 0.2 seconds and 1,000 acceleration samples for that period. In addition, fifty samples of acceleration since the start of estimation and severity values expressed as between 0 and 1 are configured as outputs. The neural network model was trained on a batch consisting of 30 input sets. Out of the fifty sets of images, forty sets were used for training and the remaining ten sets were used for verification. Specifically, a single data set consists of 3,600 images and 300,000 samples of acceleration data from a minute long CCTV video. The video was filmed at

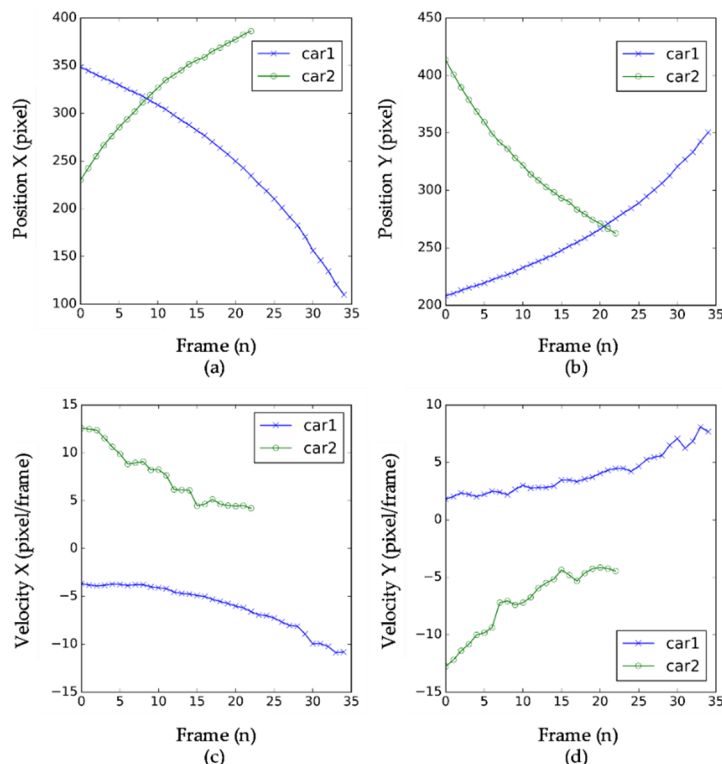


Fig. 4 Obtaining Car 1's (Fig. 3) traveling direction and current speed by calculating the recognized vehicle's position according to the time frame: (a) x - and (b) y -coordinates of the vehicle and its (c) x - and (d) y -direction velocities

the southern end of Banghwa Bridge near Incheon International Airport in South Korea.

An experiment was performed by using CCTV video of vehicles passing over the bridge as input and replacing the bridge with a cantilevered beam stationed in the laboratory to quantitatively evaluate system changes due to actual damage. Since it is practically impossible to implement local damage or changes in physical properties in a real bridge in service, we replaced the physical system of the bridge with a cantilevered beam in the laboratory. Although it is not possible to accurately measure the input caused by the movements of each vehicle over the entire bridge, the experiment was performed by replacing the magnitude or shape of the force with a mathematical model. Ultimately, when a physical system exists and the inputs and outputs applied to it can be measured, the state-space model of the system can be identified through video information. A specific force input for the cantilevered beam was obtained by using the vehicle location and speed information obtained from CCTV video images. Studies on the relationship between the force exerted by the vehicle passing over the bridge have been carried out (Tan *et al.* 1998, Kim *et al.* 2005, Yu *et al.* 2018). In this study, a simplified equation is developed by referring to the interaction between bridges and passing vehicles. The load was calculated in the form of a simplified generation function to perform a vibration test on the structure using the position and speed of the vehicle using the following equation

$$F_i(p(t), v(t)) = \exp(-k_1(p(t) - p_0)^2) * \cos(k_2 v(t) * t) \quad (1)$$

where p_0 is the mid-point of the entire bridge receiving the force. The magnitude of the force applied to the bridge appears as attenuation according to the distance between the vehicle position $p(t)$ and p_0 . This is expressed in the form of an exponential function. In addition, it is known that the frequency of the load applied to the bridge depends on the acceleration of the vehicle, which can be expressed as a sinusoidal function that is included in the simulation. Thus, force F_i is obtained for each vehicle i passing over the bridge, and the total force, F_{tot} , applied to the entire bridge is calculated as follows

$$F_{tot}(t) = \sum_{i=0}^n \text{sgn}(v) F_i(p(t), v(t)) \quad (2)$$

where sgn is a signum function to determine the direction.

3.2 Simulation using the cantilevered beam

FEM analysis was performed using the load conditions obtained in Section 3.1. As shown in Fig. 6, the applied force was excited at a node located 0.45 m from the root of the beam, and this value was recorded through the force sensor. In addition, the response at the node was calculated by assuming that it is an accelerometer mounted 5 cm from the tip of the beam. The FEM comprised Bernoulli beam elements having 20 nodes in total that were 1.1 m long, 0.1

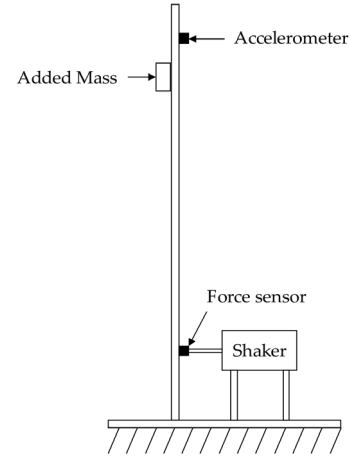


Fig. 5 A schematic of the added mass causing damage to the cantilevered beam with an electromagnetic shaker, accelerometer, and force sensor

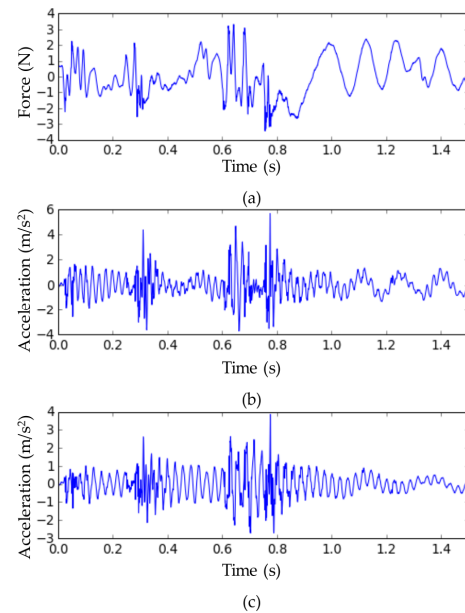


Fig. 6 Acceleration output from the FEM of the cantilevered beam: (a) input force on the beam and responses of (b) the healthy beam and (c) the fully mass-loaded beam at the accelerometer location

m wide, and $0.01 m$ thick. The elastic modulus, Poisson's ratio, and density of the model were 69 GPa, 0.33, and 7870 kg/m^3 , respectively.

Note that the mass at $0.1 m$ from the top of the FEM was modified to represent local damage in the structure. The range for varying the mass was up to 2.2 times the original, and the intervals for the variations were evenly divided into 10 steps. The acceleration response to the input load obtained through the FEM model to realize the presence of damage is shown in Fig. 7. The force input applied to the beam is shown in Fig. 7(a), while Fig. 7(b) portrays the acceleration response of a normal beam without a change in mass and Fig. 7(c) exhibits the acceleration response in the damaged state when the mass was increased by up to 2.2 times at the point of the beam shown in Fig. 6.

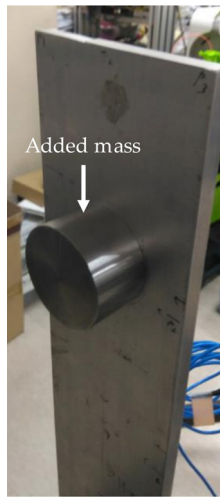


Fig. 7 Cantilevered beam with added mass in the laboratory

3.3 Experimental validation of identifying the mass-loading of the beam

An experiment was conducted to distinguish the local variations in mass applied to the cantilevered beam installed in a laboratory from vibrations caused by vehicle movements extracted from the CCTV video images. First, the cantilevered beam was excited using the input obtained from the bridge CCTV images, and then the acceleration measurements were collected. The cantilevered beam used in the experiment has the same dimensions and material properties as the model used for the FEM simulation. Similar to the simulation, an additional mass of 0.5 kg was attached 0.1 m below the tip of the beam to change the dynamic characteristics of the system and cause physical

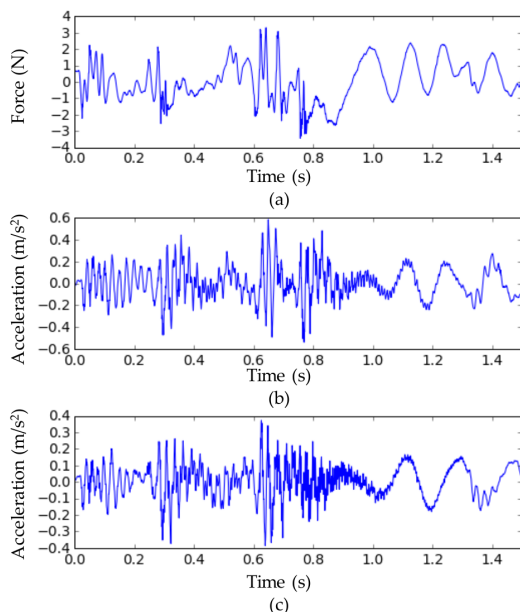


Fig. 8 Acceleration measurements from the cantilever beam in the laboratory: (a) input force on the beam and measurements on (b) the healthy beam and (c) the beam with added mass

damage to the beam (see Fig. 8). The added mass was around 15% of the total mass of the beam, which is a significant amount of variation compared to a real bridge structure. However, when considering the practical limitations of the experiment, it is still appropriate for the theoretical verification of the proposed damage detection method.

An experimental setup using accelerometers and electromagnetic shakers was constructed. Again, the location of the sensor and shaker in the structure were as depicted in Fig. 6. The vibration experiment was conducted by commanding the electromagnetic shaker and sensor using an NI-9234 dynamic signal acquisition module (National Instruments, Austin, TX, USA). To excite the cantilevered beam, a shaker from the Modal Shop (Cincinnati, OH, USA) was attached through stinger at 650 mm from the tip of the beam. The magnitude of maximum force was 67 N and the control frequency was set at 5 kHz. To measure the applied input, an Integrated Circuit Piezoelectric (ICP)-type force transducer was attached between the shaker and the beam. An ICP-type 352C33

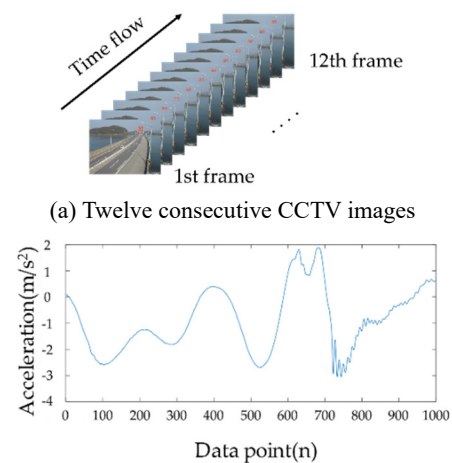


Fig. 9 Image frames and acceleration data for the training dataset

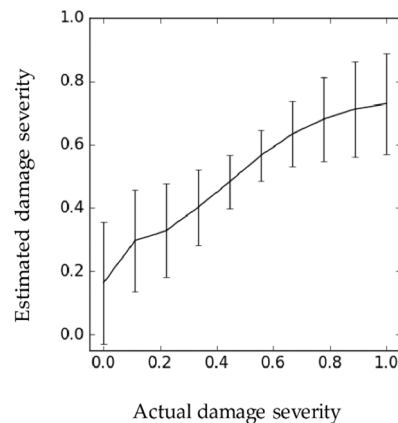
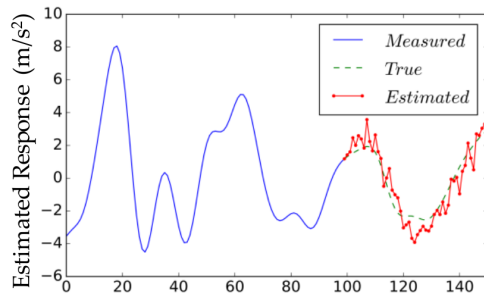
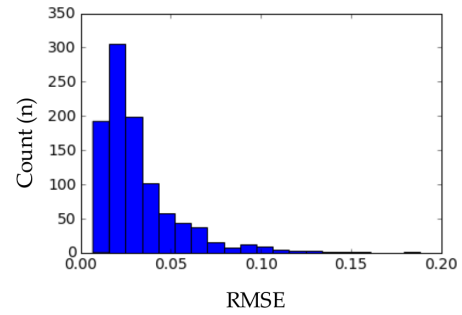


Fig. 10 Comparison between the neural network-based estimation of damage severity versus actual damage severity

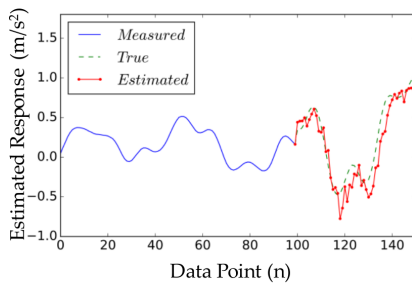


(a) The predicted and actual output values from the simulation data obtained through the trained neural network model

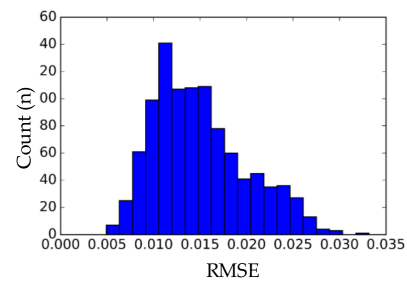


(b) A histogram of the estimated acceleration RMSE (root-mean-squared error) from the neural network

Fig. 11 Results of the neural networks obtained through the trained neural network model with simulated data



(a) The predicted and actual output using the experimental data obtained through the trained neural network model



(b) A histogram of the estimated acceleration RMSE from the neural network

Fig. 12 The trained neural network model results with experimental data

accelerometer ranging from -49.05 to 49.05 m/s^2 was used with a speed of 5 kHz and 16-bit resolution. The responses of the beam with and without mass addition to the cantilevered beam are illustrated in Fig. 9.

3.4 Structure of the neural network model and datasets

A dataset and a neural network model were constructed to train the proposed model based on the data collected through experiments. This section covers the modelling and training of the neural network for classifying mass variation in the beam structure.

3.4.1 Configuration of the datasets

A neural network model was constructed from the results of system identification using images and output obtained through experiments. The network input consisted of 12 frames of data and 1000 samples of acceleration signals that occurred in a 0.2-second interval. The output was composed of a neural network that performs two goals: estimating the acceleration signal (50 samples) after receiving the input and determining whether or not there is damage in the system. The input dataset for the configured neural network learning is described in Fig. 10.

The learning rate, which is one of the parameters used for training a neural network, was initially set to 0.005 and attenuated by 0.9 per 1000 training data items using exponential decay to adjust the learning rate. Training was performed using the Adam optimizer for network

optimization. The verification and training datasets were separated to prevent overfitting during the learning process. From a total of 50 datasets, 10 were used for validation and the remaining 40 were used for training. The GPU used for training was an NVIDIA GTX1080Ti model, and the deep learning library Tensorflow was used for training.

4. Discussions

Here, we discuss the results derived from the neural network model designed using the method described in the previous section. Fig. 11 shows the damage state estimation results obtained from the network learned through simulation. As for the degree of damage severity, the normal case without damage was set to 0 and the maximum damage state was set to 1. The damage state determined through the neural network model is expressed as error bars. The x-axis in Fig. 11 represents the severity of the actual damage in the simulation, the y-axis represents the severity of the damage estimated through the neural network, and the error bars represent one standard deviation. From the analysis results, it can be confirmed that the predicted values of the damage severity through the neural network tended to increase with the extent of damage. However, it can be seen that the extent of the damage cannot be accurately estimated when the standard deviation is relatively large.

It can be seen that the estimated range of severity was 0.0~0.3 for no actual damage and 0.6~0.9 for the full

damage case. We found that the estimated value in the vicinity of the given damage or healthy state was not clearly 1 or 0. However, we also noticed that the standard deviation was lower for damage severity from 0.4 to 0.6 compared to when the damage level was close to 0 or 1. This suggests that the success rate for the detection of medium-sized damaged areas was relatively high.

Fig. 12(a) shows a comparison between the estimated output and true values of the simulation data obtained through the trained neural network model. Note that the blue line indicates the actual acceleration measurements from the structure used as input for the neural network model, and the trained network predicted the acceleration after 100 data points. Furthermore, the red line portrays the predicted value of the structure output obtained through the neural network and the dotted green line comprises the actual measurements from the structure.

Fig. 12(b) shows a histogram of the results obtained from 1000 cases for the RMSE (root-mean-squared error) value calculated from the difference between the predicted and actual values obtained through the network model. The minimum RMSE value displayed in the histogram is zero, the maximum is 0.2, and the most highly distributed is 0.02. Nearly 90% of cases were less than 0.07 while 50% were less than 0.03. The maximum acceleration value when the vehicle crossed the bridge was around 10 m/s². In contrast, the RMSE of the predicted value was less than 0.2, indicating that the error in the estimated output from the system through the neural network was relatively small. Fig. 13(a) shows a comparison between the estimated response and actual values of the experimental data obtained through the trained neural network model. Once again, the blue line is the measured acceleration from the beam structure used as input for the network model and the trained neural network model predicted the subsequent acceleration values after 100 data points. The red line indicates the predicted values for the beam structure obtained through the neural network and the green dotted line portrays the actual measurements.

Fig. 13(b) depicts a histogram showing the RMSE from 1000 cases calculated from the difference between the predicted and actual values obtained through the trained network. The minimum RMSE in the histogram is zero, the maximum is 0.035, and the most highly distributed is 0.011. The peak of the acceleration on the beam structure when the vehicle passed over the bridge was 1 m/s². RMSE value calculated from the difference between the predicted value of the experiment and the actual acceleration was smaller than that from the simulation. However, the predicted acceleration created a bumpy line with significant errors, which means that only the trend was followed faithfully.

Table 2 reports the final results of estimating the damage presence using the proposed neural network model trained through the cantilevered structure. In the absence of damage in the beam structure, the neural network model correctly predicted that there was no damage with a probability of 85.29%, and when damage was present, it successfully predicted that with 94.01% accuracy, and the total accuracy was 89.65%. This result implies that the trained neural network can more accurately detect a faulty state than

Table 2 The results of determining the presence of damage in the beam structure obtained through the proposed neural network model

	Predicted healthy	Predicted damage	Total accuracy
Actual healthy	85.29%	14.71%	89.65%
Actual damage	5.99%	94.01%	

*Recall: 85.29%, Precision: 93.43%, F1-score: 89.17%

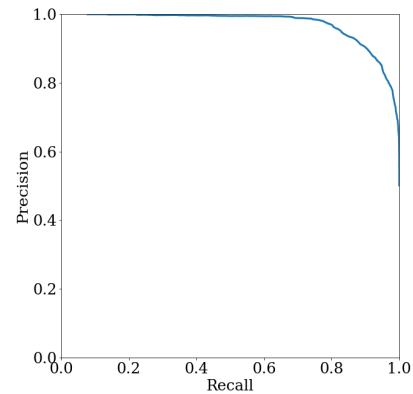


Fig. 13 Precision-recall curve of the trained neural network model with experimental data

a normal state. Also, the value of recall, the ratio of predicting actual healthy to healthy, was 85.29% and the value of precision, the ratio of actual healthy among those predicted to health, was 93.43%. Finally, the F1-score which is the harmonic mean of precision and recall is obtained as 89.17%.

Fig. 14 shows the precision-recall curve of the network model trained from the experiment data. The precision-recall curve shows the change in precision and recall according to the change of the model's threshold. Note that the value of precision is shown equal or larger than 0.98 while recall was less than 0.774. Likewise, when the recall is less than 0.98, the precision value is greater than 0.778.

In conclusion, there were more cases of false identification of the true normal state over an abnormal one than vice versa. This also means that if damage occurs in a structure, it is relatively easily detected by the proposed neural network model.

5. Conclusions

In this study, an image-based system identification technique was proposed for monitoring a bridge system based on image information from the bridge. The position and speed of vehicles on the bridge were estimated through CCTV images and the resulting force applied to the bridge structure based on the identified vehicles was generated. Simulations and experiments using the estimated force values from the images were conducted on a cantilevered beam in the laboratory. Datasets for training a neural network model were developed using the acceleration

output of the structural system obtained through the experiment and the image information from the bridge CCTV. We found that it was possible to estimate local changes in the material parameters in the beam structure by using the trained neural network model. Moreover, the proposed method successfully predicted the acceleration response of the structure. This preliminary study suggests the potential application of our proposed method for monitoring the structural integrity of bridges using image information training through deep-learning-based neural networks. We also determined that when a neural network-based correlation between the image information from the CCTV on the bridge and the input applied to the structure exists, the process of system identification can be validated even without accurate knowledge of the dynamics of the target structure. It should be noted that the proposed method is only validated in a small-scale beam model in the laboratory. It is still an open question how to transfer the findings to a real bridge problem.

Acknowledgments

This work was supported by the National Research Foundation of Korea (NRF) grant funded by the Korea government (MSIT) (No. 2018R1D1A1B07043813).

References

- Byun, Y.S., Jeong, R.G. and Kang, S.W. (2015), "Vehicle position estimation based on magnetic markers: Enhanced accuracy by compensation of time delays", *Sensors*, **15**(11), 28807-28825. <https://doi.org/10.3390/s151128807>
- Cantero, D., Arvidsson, T., O'Brien, E. and Karoumi, R. (2016), "Train-track-bridge modelling and review of parameters", *Struct. Infrastruct. Eng.*, **12**(9), 1051-1064. <https://doi.org/10.1080/15732479.2015.1076854>
- Cantero, D., Hester, D. and Brownjohn, J. (2017), "Evolution of bridge frequencies and modes of vibration during truck passage", *Eng. Struct.*, **152**, 452-464. <https://doi.org/10.1016/j.engstruct.2017.09.039>
- Chang, M. and Pakzad, S.N. (2013), "Modified natural excitation technique for stochastic modal identification", *Journal of Structural Engineering*, **139**(10), 1753-1762.
- Chang, M. and Pakzad, S.N. (2014), "Observer Kalman filter identification for output-only systems using interactive structural modal identification toolsuite", *J. Bridge Eng.*, **19**(5), 04014002. [https://doi.org/10.1061/\(ASCE\)BE.1943-5592.0000530](https://doi.org/10.1061/(ASCE)BE.1943-5592.0000530)
- Cho, S., Jo, H., Jang, S., Park, J., Jung, H.J., Yun, C.B., Spencer Jr, B.F. and Seo, J.W. (2010), "Structural health monitoring of a cable-stayed bridge using wireless smart sensor technology: data analyses", *Smart Struct. Syst., Int. J.*, **6**(5-6), 461-480. https://doi.org/10.12989/sss.2010.6.5_6.461
- Comanducci, G., Ubertini, F. and Materazzi, A.L. (2015), "Structural health monitoring of suspension bridges with features affected by changing wind speed", *J. Wind Eng. Indust. Aerodyn.*, **141**, 12-26. <https://doi.org/10.1016/j.jweia.2015.02.007>
- Deng, L. and Cai, C.S. (2009), "Identification of parameters of vehicles moving on bridges", *Eng. Struct.*, **31**(10), 2474-2485. <https://doi.org/10.1016/j.engstruct.2009.06.005>
- Deng, L., He, W., Yu, Y. and Cai, C.S. (2018), "Equivalent shear force method for detecting the speed and axles of moving vehicles on bridges", *J. Bridge Eng.*, **23**(8), 04018057. [https://doi.org/10.1061/\(ASCE\)BE.1943-5592.0001278](https://doi.org/10.1061/(ASCE)BE.1943-5592.0001278)
- Dong, H., Wen, M. and Yang, Z. (2019), "Vehicle speed estimation based on 3d convnets and non-local blocks", *Future Internet*, **11**(6), 123. <https://doi.org/10.3390/fi11060123>
- Enckell, M., Glisic, B., Myrvoll, F. and Bergstrand, B. (2011), "Evaluation of a large-scale bridge strain, temperature and crack monitoring with distributed fibre optic sensors", *J. Civil Struct. Health Monitor.*, **1**(1-2), 37-46. <https://doi.org/10.1007/s13349-011-0004-x>
- Goodfellow, I., Bengio, Y. and Courville, A. (2016), *Deep Learning*, Vol. 1, MIT press Cambridge.
- Guo, A., Jiang, A., Lin, J. and Li, X. (2020), "Data mining algorithms for bridge health monitoring: Kohonen clustering and LSTM prediction approaches", *J. Supercomput.*, **76**(2), 932-947. <https://doi.org/10.1007/s11227-019-03045-8>
- Hata, A.Y. and Wolf, D.F. (2016), "Feature detection for vehicle localization in urban environments using a multilayer LIDAR", *IEEE Transact. Intell. Transport. Syst.*, **17**(2), 420-429. <https://doi.org/10.1109/TITS.2015.2477817>
- Hou, R., Zhang, Y., O'Connor, S., Hong, Y. and Lynch, J.Á. (2015), "Monitoring and identification of vehicle-bridge interaction using mobile truck-based wireless sensors", *Proceedings of 11th International Workshop on Advanced Smart Materials and Smart Structures Technology*, 1-2.
- Imai, H., Yun, C.B., Maruyama, O. and Shinozuka, M. (1989), "Fundamentals of system identification in structural dynamics", *Probabil. Eng. Mech.*, **4**(4), 162-173. [https://doi.org/10.1016/0266-8920\(89\)90022-2](https://doi.org/10.1016/0266-8920(89)90022-2)
- Jahanshahi, M.R. and Masri, S.F. (2012), "Adaptive vision-based crack detection using 3D scene reconstruction for condition assessment of structures", *Automat. Constr.*, **22**, 567-576. <https://doi.org/10.1016/j.autcon.2011.11.018>
- James, G.H., Carne, T.G. and Lauffer, J.P. (1995), "The Natural Excitation Technique (NExT) for Modal Parameter Extraction from Operating Structures", *Modal Anal. - Int. J. Anal. Experim. Modal Anal.*, **10**(4), 260.
- Jang, S., Jo, H., Cho, S., Mechtov, K., Rice, J.A., Sim, S.H., Jung, H.J., Yun, C.B., Spencer Jr, B.F. and Agha, G. (2010), "Structural health monitoring of a cable-stayed bridge using smart sensor technology: deployment and evaluation", *Smart Struct. Syst., Int. J.*, **6**(5-6), 439-459. https://doi.org/10.12989/sss.2010.6.5_6.439
- Javadi, S., Dahl, M. and Pettersson, M.I. (2019), "Vehicle speed measurement model for video-based systems", *Comput. Electr. Eng.*, **76**, 238-248. <https://doi.org/10.1016/j.compeleceng.2019.04.001>
- Juang, J.N. (1994), *Applied System Identification*, Prentice-Hall, Inc.
- Khuc, T. and Catbas, F.N. (2018), "Structural identification using computer vision-based bridge health monitoring", *J. Struct. Eng.*, **144**(2), 04017202. [https://doi.org/10.1061/\(ASCE\)ST.1943-541X.0001925](https://doi.org/10.1061/(ASCE)ST.1943-541X.0001925)
- Kim, T. and Park, T.H. (2020), "Extended Kalman filter (EKF) design for vehicle position tracking using reliability function of radar and lidar", *Sensors*, **20**(15), 4126. <https://doi.org/10.3390/s20154126>
- Kim, C.W., Kawatani, M. and Kim, K.B. (2005), "Three-dimensional dynamic analysis for bridge-vehicle interaction with roadway roughness", *Comput. Struct.*, **83**(19), 1627-1645. <https://doi.org/10.1016/j.compstruc.2004.12.004>
- Li, J., Chen, S., Zhang, F., Li, E., Yang, T. and Lu, Z. (2019), "An adaptive framework for multi-vehicle ground speed estimation in airborne videos", *Remote Sensing*, **11**(10), 1241. <https://doi.org/10.3390/rs11101241>
- Ljung, L. (2010), "Perspectives on system identification", *Annual*

- Rev. Control*, **34**(1), 1-12.
<https://doi.org/10.1016/j.arcontrol.2009.12.001>
- Luvizon, D.C., Nassu, B.T. and Minetto, R. (2016), "A video-based system for vehicle speed measurement in urban roadways", *IEEE Transact. Intell. Transport. Syst.*, **18**(6), 1393-1404. <https://doi.org/10.1109/TITS.2016.2606369>
- Lynch, J.P., Law, K.H., Kiremidjian, A.S., Carryer, E.D., Farrar, C.R., Sohn, H., Allen, D.W., Nadler, B. and Wait, J.R. (2004), "Design and performance validation of a wireless sensing unit for structural monitoring applications", *Struct. Eng. Mech., Int. J.*, **17**(3-4), 393-408.
https://doi.org/10.12989/sem.2004.17.3_4.393
- Malekjafarian, A., McGetrick, P.J. and O'Brien, E.J. (2015), "A review of indirect bridge monitoring using passing vehicles", *Shock Vib.*, **2015**. <https://doi.org/10.1155/2015/286139>
- Mei, Q. and Gül, M. (2019), "A crowdsourcing-based methodology using smartphones for bridge health monitoring", *Struct. Health Monitor.*, **18**(5-6), 1602-1619.
<https://doi.org/10.1177/1475921718815457>
- Meng, X., Dodson, A.H. and Roberts, G.W. (2007), "Detecting bridge dynamics with GPS and triaxial accelerometers", *Eng. Struct.*, **29**(11), 3178-3184.
<https://doi.org/10.1016/j.engstruct.2007.03.012>
- Miyamoto, A., Yabe, A. and Lúcio, V.J. (2017), "Damage detection sensitivity of a vehicle-based bridge health monitoring system", *J. Phys.: Conference Series*, **842**, 012032.
<https://doi.org/10.1088/1742-6596/842/1/012032>
- Moreu, F., Kim, R.E. and Spencer Jr, B.F. (2017), "Railroad bridge monitoring using wireless smart sensors", *Struct. Control Health Monitor.*, **24**(2), e1863.
<https://doi.org/10.1002/stc.1863>
- Mufti, A.A., Tadros, G. and Jones, P.R. (1997), "Field assessment of fibre-optic Bragg grating strain sensors in the confederation bridge", *Can. J. Civil Eng.*, **24**(6), 963-966.
<https://doi.org/10.1139/97-080>
- Nagarajaiah, S., Dyke, S., Lynch, J.P., Smyth, A., Agrawal, A., Symans, M. and Johnson, E. (2008), "Current directions of structural health monitoring and control in USA", In: *Advances in Science and Technology*, Volume 56, pp. 277-286, Trans Tech Publ.
- Nayek, R. and Narasimhan, S. (2020), "Extraction of contact-point response in indirect bridge health monitoring using an input estimation approach", *J. Civil Struct. Health Monitor.*, **10**(5), 815-831. <https://doi.org/10.1007/s13349-020-00418-z>
- Pan, Y., Dong, Y., Wang, D., Chen, A. and Ye, Z. (2019), "Three-dimensional reconstruction of structural surface model of heritage bridges using UAV-based photogrammetric point clouds", *Remote Sensing*, **11**(10), 1204.
<https://doi.org/10.3390/rs11101204>
- Papageorgiou, C. and Poggio, T. (2000), "A trainable system for object detection", *Int. J. Comput. Vision*, **38**(1), 15-33.
<https://doi.org/10.1023/A:1008162616689>
- Redmon, J. and Farhadi, A. (2018), "Yolov3: An incremental improvement", ArXiv Preprint ArXiv:1804.02767.
- Smyth, A.W., Pei, J.S. and Masri, S.F. (2003), "System identification of the Vincent Thomas suspension bridge using earthquake records", *Earthq. Eng. Struct. Dyn.*, **32**(3), 339-367.
<https://doi.org/10.1002/eqe.226>
- Sochor, J., Juránek, R. and Herout, A. (2017), "Traffic surveillance camera calibration by 3d model bounding box alignment for accurate vehicle speed measurement", *Comput. Vision Image Understand.*, **161**, 87-98.
<https://doi.org/10.1016/j.cviu.2017.05.015>
- Tan, G.H., Brameld, G.H. and Thambiratnam, D.P. (1998), "Development of an analytical model for treating bridge-vehicle interaction", *Eng. Struct.*, **20**(1), 54-61.
[https://doi.org/10.1016/S0141-0296\(97\)00051-5](https://doi.org/10.1016/S0141-0296(97)00051-5)
- Tang, Z., Wang, G., Xiao, H., Zheng, A. and Hwang, J.N. (2018), "Single-camera and inter-camera vehicle tracking and 3D speed estimation based on fusion of visual and semantic features", *Proceedings of the IEEE Conference on Computer Vision and Pattern Recognition Workshops*, pp. 108-115.
- Tong, X., Yang, H., Wang, L. and Miao, Y. (2019), "The development and field evaluation of an IoT system of low-power vibration for bridge health monitoring", *Sensors*, **19**(5), 1222. <https://doi.org/10.3390/s19051222>
- Vagnoli, M., Remenyte-Priscott, R. and Andrews, J. (2018), "Railway bridge structural health monitoring and fault detection: State-of-the-art methods and future challenges", *Struct. Health Monitor.*, **17**(4), 971-1007.
<https://doi.org/10.1177/1475921717721137>
- Xiao, F., Fan, J., Chen, G.S. and Hulseley, J.L. (2019), "Bridge health monitoring and damage identification of truss bridge using strain measurements", *Adv. Mech. Eng.*, **11**(3), 1-7.
<https://doi.org/10.1177/1687814019832216>
- Yang, Y., Li, S., Nagarajaiah, S., Li, H. and Zhou, P. (2016), "Real-time output-only identification of time-varying cable tension from accelerations via complexity pursuit", *J. Struct. Eng.*, **142**(1), 04015083.
[https://doi.org/10.1061/\(ASCE\)ST.1943-541X.0001337](https://doi.org/10.1061/(ASCE)ST.1943-541X.0001337)
- Yang, L., Li, M., Song, X., Xiong, Z., Hou, C. and Qu, B. (2019), "Vehicle speed measurement based on binocular stereovision system", *IEEE Access*, **7**, 106628-106641.
<https://doi.org/10.1109/ACCESS.2019.2932120>
- Yi, T.H., Li, H.N. and Gu, M. (2013), "Wavelet based multi-step filtering method for bridge health monitoring using GPS and accelerometer", *Smart Struct. Syst., Int. J.*, **11**(4), 331-348.
<https://doi.org/10.12989/sss.2013.11.4.331>
- Yu, H., Wang, B., Li, Y., Zhang, Y. and Zhang, W. (2018), "Road vehicle-bridge interaction considering varied vehicle speed based on convenient combination of simulink and ANSYS", *Shock Vib.*, **2018**. <https://doi.org/10.1155/2018/1389628>
- Yu, Z., Shen, Y. and Shen, C. (2021), "A real-time detection approach for bridge cracks based on YOLOv4-FPM", *Automat. Constr.*, **122**, 103514.
<https://doi.org/10.1016/j.autcon.2020.103514>
- Zhang, X., Story, B. and Rajan, D. (2020), "Night Time Vehicle Detection and Tracking by Fusing Sensor Cues from Autonomous Vehicles", *Proceedings of 2020 IEEE 91st Vehicular Technology Conference (VTC2020-Spring)*, pp. 1-7.
- Zhu, D., Guo, J., Cho, C., Wang, Y. and Lee, K.M. (2012), "Wireless mobile sensor network for the system identification of a space frame bridge", *Ieee/Asme Transact. Mechatron.*, **17**(3), 499-507. <https://doi.org/10.1109/TMECH.2012.2187915>

HJ